

## ACTIVATION OF TAS<sub>2</sub> LOADED IN BLACK TITANIA NANOTUBE ARRAYS – HIGH PERFORMANCE PHOTOELECTROCHEMICAL CATHODE FOR HYDROGEN PRODUCTION

<sup>1</sup>Kamil SEVERA, <sup>1</sup>Vladislav BURAVETS, <sup>1</sup>Oleksiy LYUTAKOV, <sup>1</sup>Václav ŠVORČÍK

<sup>1</sup>Department of Solid-State Engineering, University of Chemistry and Technology, Prague,  
Czech Republic, EU, [lyutakoo@vscht.cz](mailto:lyutakoo@vscht.cz)

<https://doi.org/10.37904/nanocon.2023.4786>

### Abstract

The shift towards sustainable energy sources has generated a growing need for materials that can effectively produce and conserve alternative fuels. While platinum is known for its outstanding catalytic properties in hydrogen evolution, its scarcity presents a significant challenge. This work focuses on developing an electrode for the photoelectrochemical production of hydrogen without Pt utilization, a potential future fuel source. In particular, we introduced a novel electrode preparation method that utilizes more abundant materials, including titanium (Ti), tantalum pentoxide (Ta<sub>2</sub>O<sub>5</sub>), and gold (Au). The proposed approach begins with titanium anodization to create a TiO<sub>2</sub> nanotube array, followed by partial reduction to create a black titania structure, resulting in a high surface area with excellent light absorption. A nanostructured gold was deposited on the top of black titania and enhances light absorption, enabling the efficient use of hot electrons excited due to surface plasmon resonance. Simultaneously, controlled sulfurization of Ta<sub>2</sub>O<sub>5</sub> yields TaS<sub>2</sub> with a preferential structural modification (3R) which is later deposited on black titania/Au surface and enhances the catalytic activity of such samples. The synergistic combination of used materials, deliberate introduction of structural defects, and spatial compatibility leads to an electrode that surpasses platinum's overpotential for hydrogen evolution at high current densities. Moreover, under illumination, the prepared electrode outperforms platinum even at low current densities as low as 10 mA cm<sup>-2</sup>. This innovative approach holds promise for advancing sustainable hydrogen production and contributes to the ongoing efforts to develop alternative energy sources.

**Keywords:** Nanomaterials, TMDCs, hydrogen, water-splitting, black titania

### 1. INTRODUCTION

One remarkable aspect of the world's transition towards more sustainable and environmentally responsible energy sources lies in the search for and optimization of materials to facilitate the efficient production of renewable fuels [1]. Among these fuels, hydrogen holds a prominent position within the realm of "green" energy, as its only combustion by-product is water [2]. To meet the growing energy demand sustainably, it is imperative to produce hydrogen with the utmost efficiency, while also taking cost-effectiveness into vital consideration [3]. Electrochemical water-splitting stands as a viable method for hydrogen production, however, the current standard catalyst for hydrogen evolution, platinum, faces inherent scarcity issues [3,4].

Transition metal dichalcogenides (TMDCs) represent a group of potential alternatives to platinum. Suitable modifications of TMDCs have demonstrated their capacity to serve as excellent catalysts for hydrogen evolution in electrochemical environments [5]. While some TMDC members, such as MoS<sub>2</sub> or WS<sub>2</sub>, have been known for some time, modern preparation techniques have expanded the scope of study to wider range of TMDCs. Tantalum (IV) disulfide, in its 3R structural modification, has already displayed considerable potential as a robust catalyst [6]. One approach to enhancing the catalytic activity of TMDCs is through electrochemical activation, a process involving the tuning of TMDC flakes through cracking and basal plane modification, ultimately leading to improved hydrogen production [7,8].

However, catalysts based on flakes suffer from limitations in specific surface area, which can impact their overall performance. Combining the potential for TMDCs flakes electrochemical self-activation with the ability to load them inside nanotubular or mesh structures becomes an avenue to ensure substantial catalytic performance [3,9]. Black titania nanotube arrays have emerged as promising catalyst carriers, boasting exceptional surface density and remarkable light-absorption properties [10]. To harness light's potential in electrochemical processes to an even greater extent, the introduction of surface plasmon resonance, facilitated by various metals like gold on such surfaces, can substantially enhance catalytic activity [11].

In this study, we propose the design of a nano-structured cathode for (photo)electrochemical water-splitting. This electrode synergizes high surface density with the exceptional light-absorption capabilities of black titania nanotubes, harnesses surface plasmon resonance from a gold thin layer to utilize hot electrons, and capitalizes on the high catalytic activity of tantalum (IV) disulfide, representing a broader class of TMDCs. This paper primarily focuses on the preparation process, the investigation of morphology and composition using SEM-EDX, crystallographic analysis via XRD, and (photo)electrochemical testing of samples to evaluate their catalytic activity through Linear Sweep Voltammetry (LSVs), in comparisons to bulk Pt serving as a reference.

## 2. EXPERIMENTAL

### 2.1 Materials

Ta<sub>2</sub>O<sub>5</sub> (Sigma Aldrich, <20 µm, 99.99 %), CS<sub>2</sub> (Honeywell, ≥ 99.9 %), Ti (Goodfellow, 0.5 mm, 99.6 %), NH<sub>4</sub>F (Penta, p. a.), Glycerol (anhydrous, Lachner), H<sub>2</sub>SO<sub>4</sub> (Penta, 96 %, p. a.), Na<sub>2</sub>SO<sub>4</sub> (anhydrous, Penta, p. a.), Au target (Safina, 99.99 %), N<sub>2</sub> (Lindner, 5.0), isopropyl alcohol (Lachner, p. a.).

### 2.2 Sample preparation

The preparation of 3R-TaS<sub>2</sub> was carried out in accordance with our previous article [7]. Ta<sub>2</sub>O<sub>5</sub> was sulfurized using CS<sub>2</sub> in a quartz tube reactor at elevated temperatures. Typically, 30 mL of CS<sub>2</sub> vapor was introduced into the reactor via an Ar flow (regulated at 100 sccm by an Omega FLDA3428ST flow controller). A Nabrertherm oven was employed to heat the reactor, with a heating rate of 10 °C min<sup>-1</sup>. The reactor was brought to 650 °C and maintained at this temperature for 3 hours before cooling. The opposite end of the tube reactor was sealed with a hydroxide safety plug.

The formation of a titania nanotube array was achieved through the anodization of a titanium piece (**Figure 1A**) in a 0.27 M NH<sub>4</sub>F solution in glycerol:DI (1:1) [12]. Before anodization, the titanium piece was cleaned with isopropyl alcohol and DI water. Subsequently, it was positioned on a Teflon-coated bed mounted on a laboratory stand and secured beneath a Teflon cell using an O-ring and a magnet. Platinum served as the cathode, positioned above the sample. The anodization duration was set to 1 hour under 30 V. After anodization, the titanium piece was cleaned using isopropyl alcohol and DI water, dried, and subjected to calcination in a Nabrertherm oven at 450 °C, with a heating rate of 5 °C min<sup>-1</sup>, for 3 hours.

The partial reduction to black titania was performed electrochemically (**Figure 1B**) in a 0.1 M Na<sub>2</sub>SO<sub>4</sub> solution diluted in glycerol:DI (1:1) [10]. This process was carried out under a voltage of 15 V against a Pt counter electrode until the surface visibly darkened (typically 3 minutes). Subsequently, the electrode was cleaned using isopropyl alcohol and DI water.

In the case of samples with gold, the electrodes were coated with gold via cathodic sputtering (**Figure 1C**) using a Quorum Q300T-ES system (40 mA, 300 s, 10 Pa, ambient temperature, 20 cm from the target). After sputtering, the electrodes underwent treatment with Ar plasma (**Figure 1D**) using a Bal-Tec SCD 050 system for 300 s, with the overall power set to 15 W. The sample table was cooled with 20 °C water, and the pressure was maintained at 8 Pa throughout the treatment.

TaS<sub>2</sub> was electrophoretically deposited onto the electrode (**Figure 1E**). Prior to deposition, a suspension of TaS<sub>2</sub> in ethanol-water (19:1) was sonicated for 2 minutes. The suspension was set into a slow whirl using a magnetic plate. The sample was connected as the cathode, with a stainless-steel counter electrode. An applied potential of 50 V was used, and the deposition process lasted 5 minutes. Subsequently, TaS<sub>2</sub> was potentiostatically activated (**Figure 1F**) at - 0.4 V vs. RHE in a 0.5 M H<sub>2</sub>SO<sub>4</sub> solution using a three-electrode system connected to a PalmSens4 instrument. The activation time was set for 48 hours, with a proton-conductive membrane in an H-cell separating the Pt counter electrode from the working electrode.

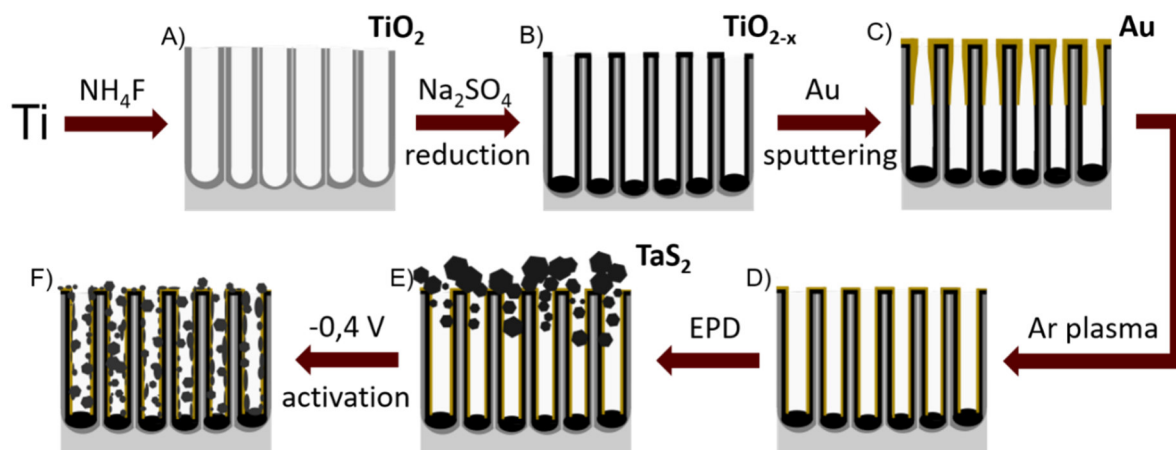


**Figure 1** Preparation route of BNT-Au-TaS<sub>2</sub>, A) anodization of Ti, B) partial reduction of TiO<sub>2</sub> nanotube array, C) Au cathodic sputtering, D) Ar plasma treatment, E) electrophoretic deposition of TaS<sub>2</sub>, F) activation of TaS<sub>2</sub> on BNT-Au surface under -0.4 V vs RHE

### 2.3 Measurement techniques

SEM-EDX was performed on LYRA3 GMU (Tescan, CZ); XRD diffractograms were obtained on X'Pert<sup>3</sup> Powder (Malvern PANalytical, NL,  $\lambda_{\text{Cu K}\alpha} = 1.54 \text{ \AA}$ ); power source for anodization, electrochemical reduction, electrophoretic deposition and photo-electrochemistry (Manson HCS-3104); potentiostat (PalmSens4); electrochemical H-cell with proton-conducting membrane; Ag/AgCl (3M KCl) referential electrode; LEDs controlled by Thorlabs LEDD1B (12 V forward, 1 A) : 455 nm, 530 nm, 660 nm; Xe lamp (7.3 V, 3 A).

## 3. RESULTS AND DISCUSSION

**Figure 2** presents the SEM results depicting the surface morphology at distinct stages of the electrode substrate preparation route. In **Figure 2A**, we observe the TiO<sub>2</sub> nanotube array, achieved through anodization at 30 V for 1 hour, followed by calcination.

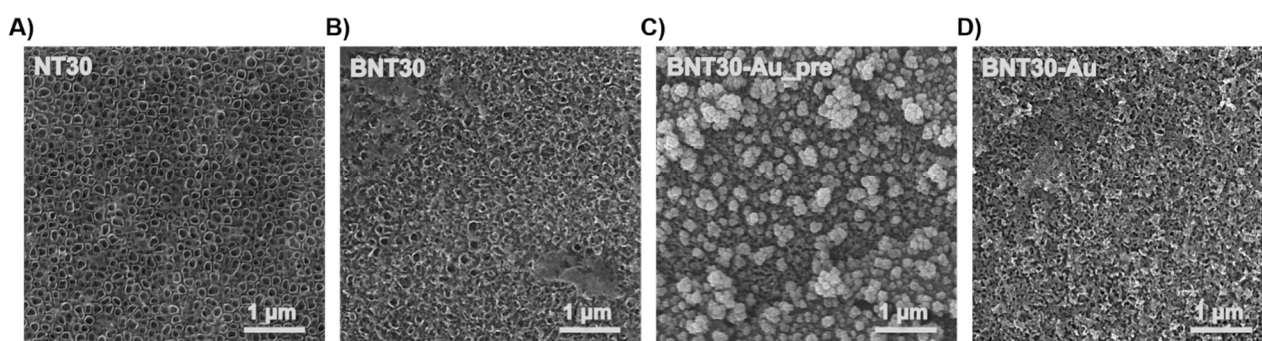


**Figure 2** SEM results of A) electrode anodised at 30 V and calcined at 450 °C; B) partially reduced electrode; C) Au sputtered electrode; D) Ar plasma treated electrode

Under these conditions, the pore size measures approximately 140 nm. The progressive impact of the partial reduction of  $\text{TiO}_2$  is depicted in **Figure 2B**. While the structure exhibits noticeable distortion, the characteristic nanotubular array is still discernible. In **Figure 2C**, we observe a partially reduced nanotube array of anodized titania, which has been sputtered with Au.

It is evident that the Au clusters obstruct the inner surface of the black titania nanotubes. Consequently, the electrode's surface was treated with Ar plasma, as demonstrated in **Figure 2D**. It is apparent that this treatment leads to homogeneous redistribution of matter on the surface.

The diffractogram in **Figure 3A** presents measurements of both plain  $\text{Ta}_2\text{O}_5$  powder, utilized as a precursor, and  $\text{TaS}_2$ , indicating that the chosen conditions for  $\text{TaS}_2$  preparation yield a coordination structure of 3R [6,7]. Changes observed during the preparation of the black titania substrate are illustrated in **Figure 3B**.

Specifically, it is evident that calcination (NT30\_c) accentuates the most intense anatase peak, (101), at  $25.3^\circ$ . This indicates an increase in crystallinity during annealing, demonstrating that the selected temperature favors the preferential growth of anatase over rutile phase [12]. Importantly, partial reduction (BNT30) leads to the appearance of distinct new peaks at  $28.4^\circ$  and  $29.3^\circ$ , which can be attributed to oxygen-vacant black titanium oxide. This form of titanium dioxide is renowned for its strong light absorption, narrower band gap, and higher catalytic activity compared to pure anatase [9, 10].

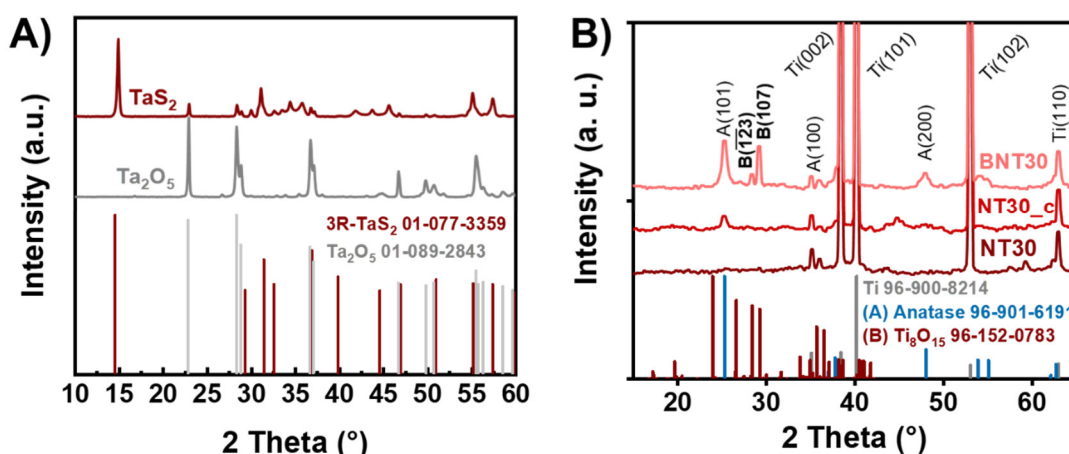


**Figure 3** XRD diffractograms of A)  $\text{TaS}_2$  after sulfurization; B) anodised titania before and after calcination and after partial reduction

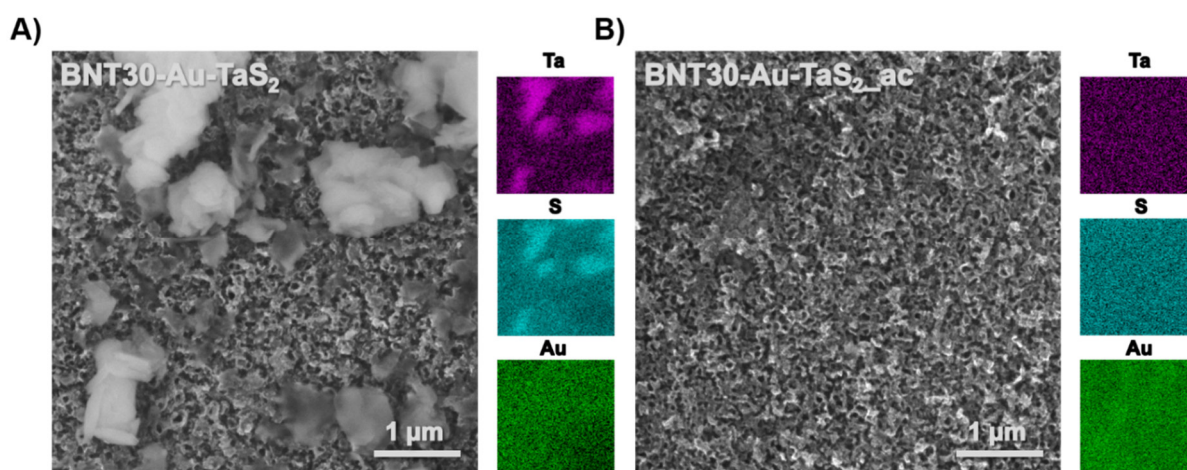


**Figure 4** SEM-EDX results of surface A) before and B) after  $\text{TaS}_2$  activation process



SEM-EDX analysis was conducted on samples both after electrophoretic deposition (**Figure 4A**) and following the electrochemical activation of TaS<sub>2</sub> on the previously described substrate. Notably, large 2D hexagonal flakes of TaS<sub>2</sub> are clearly visible on top of the nanotube array. When comparing these results to those obtained after the 48-hour electrochemical activation process (**Figure 4B**), it becomes evident that the distribution of TaS<sub>2</sub> has become more uniform, and the particle size has markedly decreased. This observation aligns well with the proposed activation mechanism, which involves the cracking of large flakes and the chemical tuning of the basal plane of these flakes [7,8].

As illustrated in **Figure 5A**, there is a noticeable increase in catalytic activity when an Au interlayer is introduced. This is likely attributed to the enhanced electron transfer to the TaS<sub>2</sub> catalyst [9,11]. However, after 48 hours of electrochemical activation, the difference in LSV curves becomes less pronounced. This suggests that the primary catalyst on the electrode's surface is, in fact, TaS<sub>2</sub>, and its structural and electron changes via electrochemical activation lead to a significantly reduced overpotential for hydrogen evolution. It is noteworthy that at higher current densities ( $> 40 \text{ mA cm}^{-2}$ ), the overpotential for HER on the electrode with an Au interlayer is lower than that of platinum (although the onset potential for platinum is still lower). This can be attributed to the finely-tuned nano-structuring of the electrode's surface, which has a remarkable impact on its catalytic activity.

**Figure 5B** demonstrates that the electrode's electrochemical performance can be significantly enhanced with illumination. The greatest improvement in catalytic activity is achieved when using a Xe lamp that mimics the emission spectra of the Sun. This highlights the electrode's high capability in utilizing photons of various wavelengths for its electrochemical activity [11].

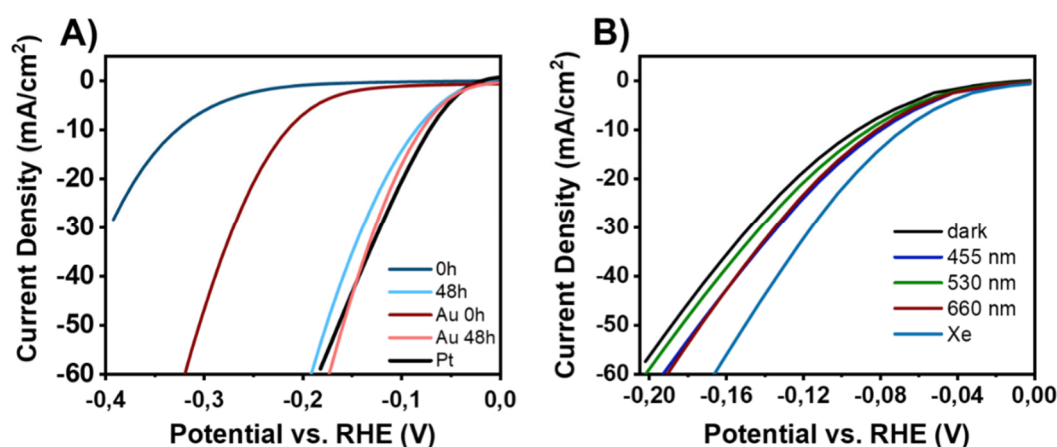


**Figure 5** Linear sweep voltammetries performed in 0.5 M H<sub>2</sub>SO<sub>4</sub> of A) before and after activation of electrodes for electrode with and without Au; B) photoelectrochemical analysis with various light sources of sample BNT30-Au-TaS<sub>2</sub>\_ac

#### 4. CONCLUSION

In this study, we introduced a novel electrode design for efficient hydrogen evolution under photoelectrochemical conditions. Our electrode combines a black titania nanotube array, achieved through titanium anodization, calcination, and partial electrochemical reduction, with a thin gold film and tantalum (IV) disulfide flakes. Through electrochemical activation at a constant negative potential, we observed a remarkable reduction in the overpotential required for the hydrogen evolution reaction. This reduction exceeded that of a bulk platinum electrode, particularly at high current densities exceeding  $40 \text{ mA cm}^{-2}$ . Furthermore, our electrode exhibited significantly improved catalytic activity when illuminated by various light sources. The best performance was achieved under Xenon lamp illumination, attributed to the electrode's broad light-absorption spectrum and the additional heating effect. In summary, our designed electrode not only shows

promise for efficient hydrogen evolution in photoelectrochemical settings but also outperforms conventional bulk platinum electrodes, particularly at high current densities. These findings hold significant potential for advancing clean energy technologies and warrant further exploration and optimization.

## ACKNOWLEDGEMENTS

***This work was supported by GACR under the project number 23-05197S***

## REFERENCES

- [1] WANG, F., R. SWINBOURN, and C.E. LI. Shipping Australian sunshine: Liquid renewable green fuel export. *International Journal of Hydrogen Energy*. 2023, vol. 48, no. 39, pp. 14763-14784.
- [2] AHMED, A., et al. Hydrogen fuel and transport system: A sustainable and environmental future. *International Journal of Hydrogen Energy*. 2016, vol. 41, no. 3, pp. 1369-1380.
- [3] ZHANG, C., et al. High-throughput production of cheap mineral-based two-dimensional electrocatalysts for high-current-density hydrogen evolution. *Nature Communications*. 2020, vol. 11, no. 1, pp. 3724.
- [4] ZABELIN, D., et al. Creation and Plasmon-Assisted Photosensitization of Annealed Z-Schemes for Sunlight-Only Water Splitting. *ACS Applied Materials & Interfaces*. 2023, vol. 15, no. 24, pp. 29072-29083.
- [5] FU, Q., et al. 2D Transition Metal Dichalcogenides: Design, Modulation, and Challenges in Electrocatalysis. *Advanced Materials*. 2021, vol. 33, no. 6, pp. 1907818.
- [6] FENG, Y., et al. 3R TaS<sub>2</sub> Surpasses the Corresponding 1T and 2H Phases for the Hydrogen Evolution Reaction. *The Journal of Physical Chemistry C*. 2018, vol. 122, no. 4, pp. 2382-2390.
- [7] BURAVETS, V., et al. Beyond the Platinum Era—Scalable Preparation and Electrochemical Activation of TaS<sub>2</sub> Flakes. *ACS Applied Materials & Interfaces*. 2023, vol. 15, no. 4, pp. 5679-5686.
- [8] CHIA, X., et al. Precise Tuning of the Charge Transfer Kinetics and Catalytic Properties of MoS<sub>2</sub> Materials via Electrochemical Methods. *Chemistry – A European Journal*. 2014, vol. 20, no. 52, pp. 17426-17432.
- [9] CHENG, Y., et al. In situ electrochemical reduced Au loaded black TiO<sub>2</sub> nanotubes for visible light photocatalysis. *Journal of Alloys and Compounds*. 2022, vol. 901, p. 163562.
- [10] LIU, X., et al. Progress in Black Titania: A New Material for Advanced Photocatalysis. *Advanced Energy Materials*. 2016, vol. 6, no. 17, p. 1600452.
- [11] GODDETI, K.C., et al. Three-dimensional hot electron photovoltaic device with vertically aligned TiO<sub>2</sub> nanotubes. *Scientific Reports*. 2018, vol. 8, no. 1, p. 7330.
- [12] ROY, P., S. BERGER, and P. SCHMUKI. TiO<sub>2</sub> Nanotubes: Synthesis and Applications. *Angewandte Chemie International Edition*. 2011, vol. 50, no. 13, pp. 2904-2939.